Fault Detection and Localization in Transmission Lines with a Static Synchronous Series Compensator

Enrique REYES-ARCHUNDIA, José Leonardo GUARDADO, Edgar Lenymirko MORENO-GOYTIA, José Antonio GUTIERREZ-GNECCHI, Fernando MARTÍNEZ-CÁRDENAS
Instituto Tecnológico de Morelia, Ave. Tecnológico 1500, 58120, Morelia, México
ereyes@itmorelia.edu.mx

***Abstract*—This paper proposes a fault detection and localization method for power transmission lines with a Static Synchronous Series Compensator (SSSC). The algorithm is based on applying a modal transformation to the current and voltage signals sampled at high frequencies. Then, the wavelet transform is used for calculating the current and voltage traveling waves, avoiding low frequency interference generated by the system and the SSSC. Finally, by using reflectometry principles, straightforward expressions for fault detection and localization in the transmission line are derived. The algorithm performance was tested considering several study cases, where some relevant parameters such as voltage compensation level, fault resistance and fault inception angle are varied. The results indicate that the algorithm can be successfully be used for fault detection and localization in transmission lines compensated with a SSSC. The estimated error in calculating the distance to the fault is smaller than 1% of the transmission line length. The test system is simulated in PSCAD platform and the algorithm is implemented in MATLAB software.**

***Index Terms*— fault location, flexible AC transmission systems, transmission lines, wavelet transform, waves propagation.**

I. INTRODUCTION

The introduction of power electronics in transmission networks has increased significantly over the last two decades. Some examples of these new developments are the extensive use of power converters and Flexible AC Transmission Systems (FACTS) under the framework of the smart grid concept.

These developments also represent new challenges to other electrical engineering areas. For example, in power system protection is of great interest to assess the impact that dynamic compensators may have on conventional protection schemes. This is because FACTS controllers, like the Thyristor Controlled Series Compensator (TCSC), can modify the impedance measured by conventional distance relays [1-2]. This is also true for the case of Static Compensators (STATCOM); for example, in [3-4] the authors demonstrate that these devices have an impact in the tripping characteristic of protective relays. On the other hand, in [5-6] the authors have demonstrated that the SSSC also affects the tripping characteristics of distance relays. From the above, power electronic devices can have an impact in the characteristics of modern protection schemes.

This work was supported by CONACYT, DSA and the Tecnológico Nacional de México.

Digital Object Identifier 10.4316/AECE.2015.03003

The development of new protection algorithms for power transmission networks with power electronic devices in service is a need. In [7], Ghorbani *et al* proposed a method for protecting power transmission lines with a SSSC in service. This approach is based on compensating the zero sequence voltage injected by the SSSC. Although this method was proposed initially for fault detection and localization, its main drawback is the long times required (≈ 60 ms) for fault localization, as shown in [8].

In [9], Zonkoly and Desouky used optimization techniques and the wavelet transform based in entropy in order to discriminate whether the fault is before or after the SSSC in a series compensated transmission line. It should be mentioned that this approach was not capable to pin point the precise distance to the fault in order to facilitate repairs and service restoration.

In general, fault detection and localization in transmission lines with a SSSC device in service is a great challenge, because this device injects voltage and current to the transmission network which may lead to over-reach in conventional distance relay and therefore malfunctioning. In order to overcome these difficulties, new alternative techniques are being continuously explored.

A trend of development is based on sampling at high frequencies the faulted signals for further analysis and processing. Thus, after fault inception two electromagnetic waves are produced which travel in both directions along the transmission line. Relays at both ends of the line measure these high frequency pulses (traveling waves), and by using reflectometry principles and digital signal processing techniques, the exact distance to the fault can be calculated. This approach requires high frequency sampling rates (>20 kHz).

In addition, the Wavelet Transform (WT) is used quite frequently to discriminate the high frequency components due to the transient fault period from the low frequency components generated by power electronic devices, since both signals are superimposed to the power frequency signal (50-60 Hz). The WT has been successfully applied for fault detection and localization in overhead transmission lines [10], cables [11], distribution lines [12], STATCOM and TCSC compensated transmission lines [13-14]. As far as the authors know, never before this approach has been applied successfully to transmission lines with a SSSC in service.

This paper proposes a fault detection and localization

method based on the traveling waves produced during fault events in a SSSC compensated transmission line. The paper is organized as follows: first, the interaction between harmonic frequencies generated by the TCSC and the travelling wave pattern produced during a fault event is analyzed. Second, the proposed protection algorithm is presented. Then, the proposed algorithm is validated and several studies on transmission lines involving faults and the SSSC are presented. Finally the paper conclusions are given.

II. Analysis of Traveling Waves in Transmission Lines with a SSSC

The SSSC controller is connected in series with the transmission line. The device behaves as a voltage source (V_q) in quadrature with the line current. Since the SSSC can increase or decrease the voltage across the line, this facilitates the control of power transfer across the line. Fig. 1 shows the equivalent circuit for a SSSC [15].

During a fault event in the transmission line, steep fronted pulses traveling in opposite directions are generated at the Faulted Point (FP). These pulses are traveling waves in the transmission line. From Fig.1, observe that at least a traveling wave get through the SSSC before reaching the line end. Since the transmission line and the SSSC have different impedances, some changes in the pattern of traveling wave propagation can be expected. In particular, two effects are relevant to this study: a) travelling wave attenuation and b) frequency overlap between the low frequency harmonics generated by the SSSC controller and the high frequency components of traveling waves.

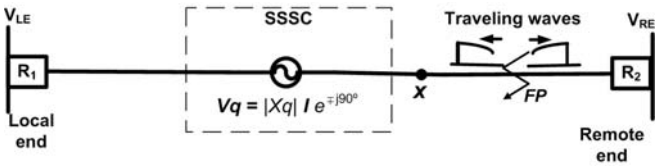

Figure 1. SSSC equivalent circuit and traveling waves

A. Traveling waves magnitude

In general, the voltage at any point "x" along the transmission line is given by [16]:

$$v_x = (V_- e^{-\gamma x} + V_+ e^{+\gamma x}) \tag{1}$$

where γ is the transmission line propagation coefficient, $V_- e^{-\gamma x}$ is the incident wave and $V_+ e^{+\gamma x}$ is the reflected wave from the remote end, V_- and V_+ are coefficients depending on the boundary conditions in the line.

Observe in Fig. 1 that the SSSC is located at the middle of the line. Then, for a fault between the remote end and the SSSC, the traveling waves reach the relay (R_2) at the remote end undisturbed. There is no need to take any remedial action in this case. However, traveling waves in the direction of the local end have to get through the SSSC before reaching the relay (R_1). The reflection coefficient ρ_v in the transition point is [16]:

$$\rho_v = \frac{V_+ e^{+\gamma x}}{V_- e^{-\gamma x}} = \frac{Z_x - Z_0}{Z_x + Z_0} \tag{2}$$

where Z_x is the SSSC impedance and Z_0 is the characteristic impedance of the line. The impedance seen by the traveling wave at the SSSC boundary is given by:

$$Z_x(s) = Z_0 + jX_q \tag{3}$$

Substituting (3) in (2) leads to:

$$\rho_v = \frac{jXq}{jXq + 2Z_0} \tag{4}$$

In a given time instant, the synchronous voltage source in Fig. 1 can be substituted by an equivalent series capacitor leading to the same effect, an increase on line voltages and power transfer. Thus, equation (3) can be rewritten as:

$$Z_x(s) = Z_0 - jX_C \tag{5}$$

where X_c is the apparent capacitive reactance of the synchronous voltage source. The reflection coefficient ρ_v can be obtained by substituting (5) into (2):

$$\rho_v = \frac{-jX_C}{2Z_0 - jX_C} \tag{6}$$

Now, let us consider the following illustrative example: a 230 kV transmission line, 360 km length and the typical parameters presented in [17]. The inductance and capacitance are respectively:

For positive sequence:

$$L_1 = 0.0008H/km \tag{7}$$
$$C_1 = 1.402e^{-8}F/km$$

For zero sequence:

$$L_0 = 0.0027H/km \tag{8}$$
$$C_0 = 8.82e^{-9}F/km$$
$$Z_0 = \sqrt{\frac{L_0}{C_0}} = 553\Omega$$

The total line inductive reactance can be calculated by substituting L_1 in (9):

$$X_L = \omega L_l T_{LL} \tag{9}$$

where T_{LL} is the transmission line length. Thus:

$$X_L = 2\pi(60Hz)(0.0008H/km)(360km) = 108.75\ \Omega$$

By considering a 50% reactive compensation, the capacitive reactance at 60 Hz and its respective capacitance are:

$$X_C = \frac{X_L}{2} = 54.28\Omega \tag{10}$$

$$C = \frac{1}{\omega X_C} = \frac{1}{2\pi(60Hz)54.28\Omega} = 0.0029F \tag{11}$$

Once the value of C is calculated, it is possible to obtain the reflection coefficient ρ_v in (6), substituting X_C by $1/\omega C$.

$$\rho_v = \frac{-j}{2Z_0\omega C - j} \tag{12}$$

From (12), the ρ_v can be plotted by varying the value of frequency, see Fig. 2. Observe that traveling waves get through the SSSC without any significant change in magnitude. This is because the reflection coefficient is very small at the high frequencies typical of traveling wave components.

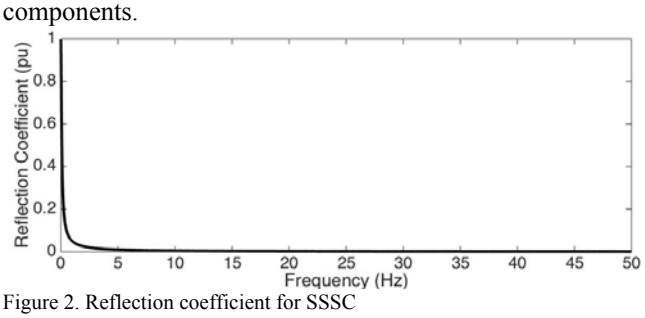

Figure 2. Reflection coefficient for SSSC

B. Harmonic interaction between the SSSC and traveling waves

Let us consider a conventional six-pulse SSSC. According to [18], the harmonic voltages components are the 3º, 5º and 7º, which correspond to 180, 300 and 420 Hz. Thus, the voltage in phase A, including the fundamental frequency, is represented by:

$$v_a = \frac{4}{\pi}\left(\frac{Vd}{2}\right)\left[\cos\omega t - \frac{1}{3}\cos 3\omega t + \frac{1}{5}\cos 5\omega t - \frac{1}{7}\cos 7\omega t + ...\right] \quad (13)$$

In other words, the SSSC is injecting continuously to the line low frequency harmonics. Also, during a fault event in the line, additional high frequency components are generated i.e. traveling waves. These low and high frequency signals are superimposed on the fundamental frequency (50-60 Hz), and the main concern here is about the impact that these low frequency components may have in the complex pattern of traveling wave reflections and refractions. If the traveling wave pattern is severely distorted, then this information cannot be used for protective relay applications.

The Wavelet Transform (WT) is the natural tool to analyze these complex interactions between low and high frequency components. However, when using the WT for solving this sort of problems, care must be taken with the detail components, cD_n, used for protective relaying algorithms. This is because the frequency range of some cD_n may fall in the range of low frequencies produced by the SSSC. For example, Table I shows the cD_n used in this paper considering a sampling rate of 80 kHz and mother wavelet *db4*. Observe that each cD_n is associated with a certain range of frequencies.

TABLE I. FREQUENCY RANGES OF CD_N

cD_n	Frequency ranges
cD_1	20 kHz to 40 kHz
cD_2	10 kHz to 20 kHz
cD_3	5 kHz to 10 kHz
cD_4	2.5 kHz to 5 kHz
cD_5	1.25 kHz to 2.5 kHz
cD_6	625 Hz to 1.25 kHz
cD_7	312.5 Hz to 625 Hz
cD_8	156 Hz to 312 Hz
cD_9	78 Hz to 156 Hz
cD_n	20 kHz to 40 kHz

From Table I, the SSSC harmonics may overlap cD_7 and cD_8. Therefore, to avoid any interference is desirable to use the low-level detail components, cD_1 for instance.

In order to show that SSSC generated harmonics can be effectively discriminated from fault signals, let us consider the system shown in Fig. 3. The arrangement consists of a SSSC in the middle of the 345 kV transmission line. A three-phase fault is applied at 300 km from the local end.

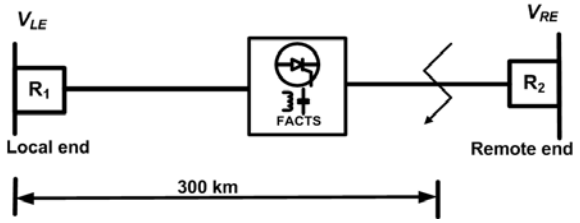

Figure 3. Three phase fault to ground at 300 km from R_1.

The fault is applied at 0.3 s and two cases are analyzed, with and without SSSC. The sampling rate is 80 kHz and the mother wavelet used is *db4*. The results obtained after using cD_1 and cD_8 are shown in Fig. 4.

The results presented in Fig. 4c show that the harmonic content generated by the SSSC is still important in cD_8. This is evident because of the differences between the cases with and without SSSC.

On the other hand, the use of cD_1 in the WT shows practically no changes between both cases: with and without SSSC, see Fig 4b. This demonstrates that the use of a cD_n with a higher frequency range provides an effective separation between the low and high frequency components.

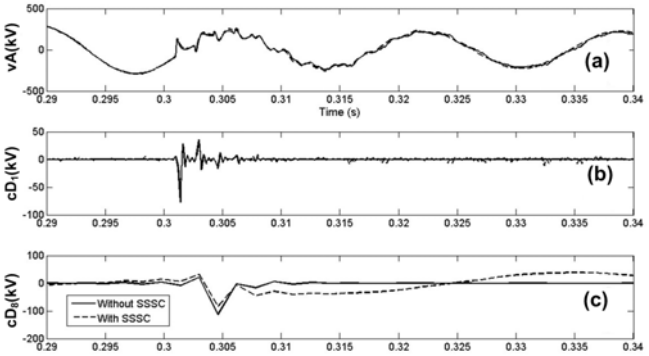

Figure 4. a) Three phase fault, b) cD_1 results and c) cD_8 results.

III. ALGORITHM FOR FAULT DETECTION AND LOCALIZATION

The algorithm for fault detection and localization is based in sampling the power signal at high frequency, 80 kHz. This information is processed and analyzed in order to extract the relevant information from cD_1. Fig. 5 shows the algorithm structure.

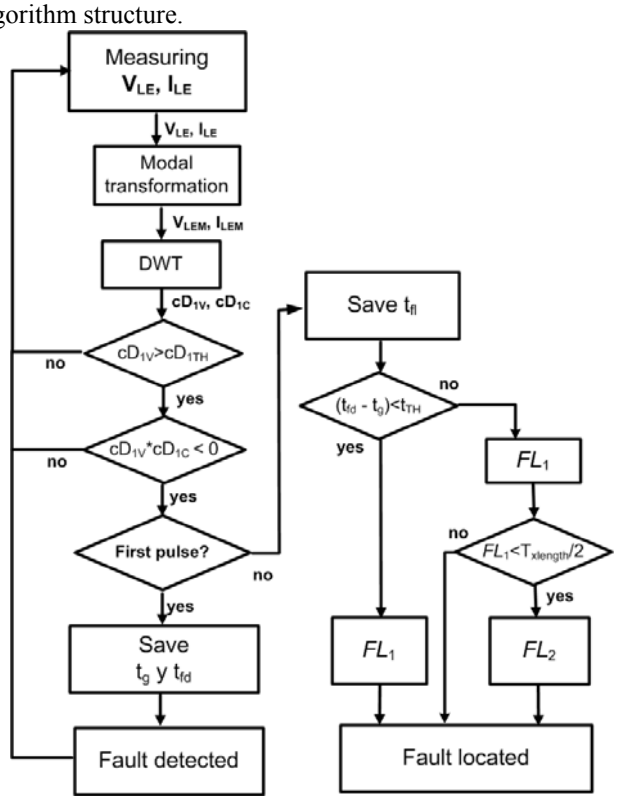

Figure 5. Fault detection and localization algorithm.

The main steps can be summarized as follows:

1. Pre-processing. Prior to obtaining the cD_1 from the power signal, the first step consists in applying a modal

transformation to eliminate mutual coupling between phases. Clarke transformation was used throughout this work. Thus, signals in the phase domain are translated to the modal domain

2. Obtaining cD_1. The WT is applied to the measured signals and two coefficients of detail are obtained, voltage (cD_{1V}) and current (cD_{1C}). The peak magnitudes of these coefficients are used for fault detection and localization
3. If $cD_{1V} > cD_{1TH}$ then the fault is detected. The voltage magnitude of the traveling wave is continuously compared with a threshold value (cD_{1TH}), normally 5% of peak voltage, in order to detect the presence of faults in the line. The current traveling wave is used to verify the wave direction. When current and voltage polarities of traveling waves are different, then the traveling wave is valid to be used for protecting the line, otherwise the traveling wave was produced behind the relay position.
4. The distance to the fault can be calculated when the peak value of cD_{1V} is greater than cD_{1TH} for the second pulse. Then, equations (14) or (15) can be used depending on the time elapsed between traveling waves in the aerial and ground mode [19]. For instance:

   If (t_g-$t_{fd} < t_{TH}$) then use FL_1:

$$FL_1 = k_v(t_{fl} - t_{fd})/2 \quad (14)$$

   If (t_g-$t_{fd} > t_{TH}$) and ($FL_1 < T_{LL}/2$) then use FL_2:

$$FL_2 = T_{LL} - FL_1 \quad (15)$$

   where FL_1 is the distance to the fault and FL_2 is also the distance to the fault but only if the fault is located after the SSSC, k_v is the speed of travelling waves in the air (2.997x105 km/s), t_{fl} is the time of arrival of the second peak of the aerial model to the relay position R_1, t_{fd} is the time of arrival for the first traveling wave aerial model to the relay position R_1 and T_{LL} is the length of the transmission line (km). On the other hand, t_g is the arrival time of traveling wave ground mode to R_1, t_{TH} is a time interval between t_g and t_{fd}, when the fault occurs at the middle of the line.

In order to illustrate the effectiveness of the proposed algorithm, let us consider a fault applied in the transmission line beyond the position of the FACTS device, as shown in Fig. 6.

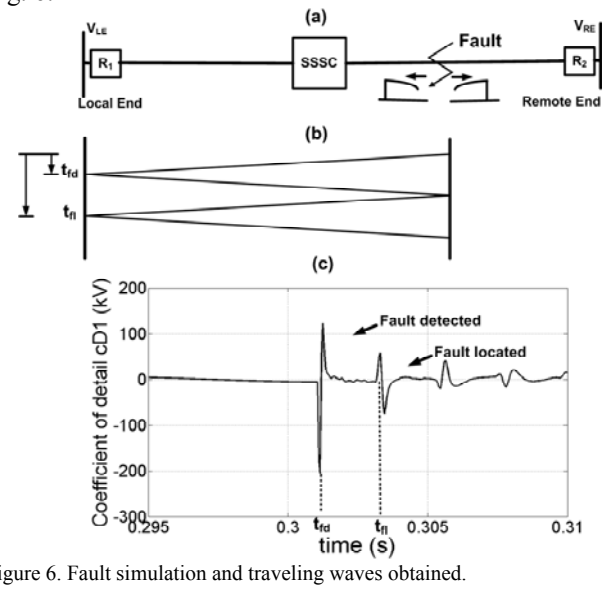

Figure 6. Fault simulation and traveling waves obtained.

Under these conditions, the traveling wave pulses travel from the fault to R_1 and arrive at the local end at time t_{fd}. The traveling wave is reflected back and returns to the faulted point, only to be reflected back again, arriving to R_1 for the second time at t_{fl}, Fig. 6b. The pulses generated after fault inception are shown in Fig. 6c. Observe the correspondence between the arrival time in 5b and those obtained in 5c. Thus, the faults was applied at 0.3 s, the first pulse is detected at time t_{fd}=0.301 s and the second pulse arrives at the local end at time t_{fl}=0.303 s. By using (16), the distance to the fault is calculated at 299.7 km from R_1.

IV. Study Cases

The 12-buses power grid shown in Fig. 7 was selected to analyze several cases of study. The system has 6 buses at 230 kV, 2 buses at 345 kV and 4 buses at 22 kV [17]. The electrical grid and the proposed algorithm were simulated in PSCAD®. The SSSC is located between buses 1 and 6, at the middle. The transmission line length is 300 km. This power grid has been used by previous authors for the analysis of traveling wave relays without FACTS devices [20].

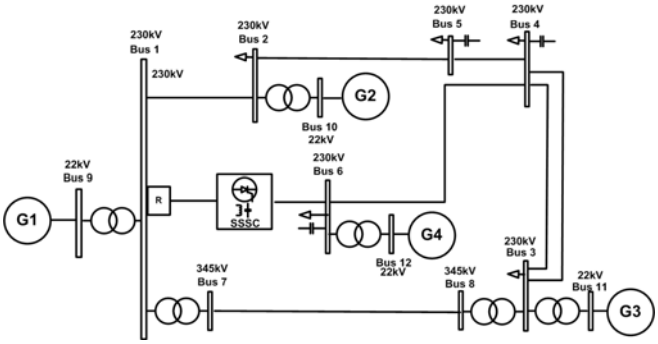

Figure 7. 12-node electrical grid with a SSSC.

A. Case I. Fault Localization

Fig. 8 shows the signals observed during a fault event using cD_1. The fault was applied at 180 km from node 1, where the algorithm is embedded in relay *R*. The impulses observed at 0.3006s are measured at bus1, and both current and voltage pulses have different polarity. The algorithm validates correctly the polarity of both signals and calculates the distance to the fault at 180.1 km.

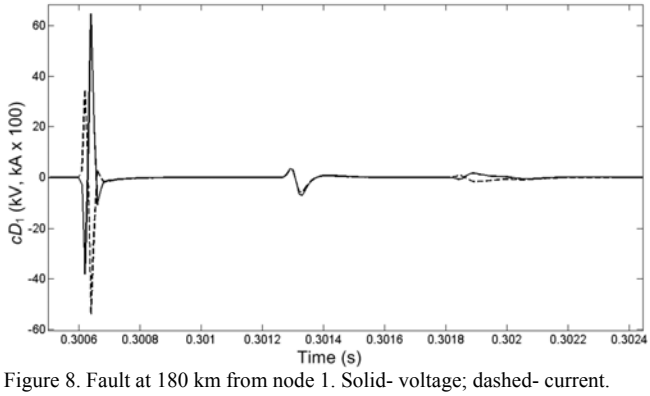

Figure 8. Fault at 180 km from node 1. Solid- voltage; dashed- current.

In order to validate the general performance of the algorithm for fault localization, several types of faults were simulated along the transmission line. A summary of these results is presented in Table II. Observe that regardless of the type of fault, the algorithm correctly calculates the

distance to the fault. For instance, for a fault AB-G at 150 km from node 1, the algorithm calculates a distance of 151.87 km (i.e. a difference of 1.87 km) which is basically an error of 0.62%, considering (16):

$$\text{Error} = (\text{calculated value} - \text{actual value})/\ T_{LL} \qquad (16)$$

TABLE II. DISTANCE TO THE FAULT FOR SEVERAL FAULT TYPES

Type of Fault	Fault applied at (km)					
	60	120	150	180	240	300
	Fault calculated at (km)					
A-G	60.01	120.03	151.87	181.88	241.86	300.01
B-G	60.01	121.86	151.87	181.88	241.86	300.01
C-G	60.01	121.86	151.87	181.88	241.86	301.88
AB-G	60.01	120.03	151.87	180.04	240.06	300.01
AC-G	60.01	120.03	151.87	178.13	241.86	301.88
BC-G	60.01	120.03	148.13	181.88	238.12	301.88
ABC-G	60.01	120.03	150.73	180.04	241.86	300.01
AB	60.01	120.03	151.87	180.04	240.06	300.01
AC	60.01	120.03	150.73	180.04	240.06	300.01
BC	60.01	120.03	150.73	180.04	238.12	298.14
ABC	60.01	120.03	150.73	180.04	241.86	300.01

B. Case II. SSSC Compensation Level

In order to validate the effect of the compensating voltage applied in series with the transmission line, different voltages magnitudes were considered. The voltages considered are proportional to the transmission line level of capacitive reactance compensation. Table III shows the results obtained due to an A-G fault at 180 km from *R* considering five different compensation voltages.

The results presented in Table III show that the level of compensation does not affect the algorithm accuracy; this is explained by the fact that the use of cD_1 effectively isolates the SSSC from traveling waves.

TABLE III. EFFECT OF LEVEL OF COMPENSATION

Compen-sation Voltage (pu)	Fault applied at (km)					
	60	120	150	180	240	300
	Fault calculated at (km)					
0.0	60.01	120.03	151.87	181.88	241.86	300.01
0.01	60.01	120.03	151.87	181.88	241.86	300.01
0.02	60.01	120.03	151.87	181.88	241.86	300.01
0.03	60.01	120.03	151.87	181.88	241.86	300.01
0.04	60.01	120.03	151.87	181.88	241.86	300.01
0.05	60.01	120.03	151.87	181.88	241.86	300.01
0.06	60.01	120.03	151.87	181.88	241.86	300.01

C. Case III. Fault Resistance

The fault resistance (R_f) can modify significantly the calculated distance to the fault in conventional relays [21]. In order to evaluate the impact of this parameter in the algorithm performance, several cases were analyzed as shown in table IV.

In average, the error in calculating the distance to the fault is smaller than 0.7% for all types of faults. It is worth to mention that these errors are also dependent on the sampling frequency. For instance, the highest error is smaller than 0.6 % for a sampling frequency of 100 kHz and 0.8% for a sampling frequency of 60kHz.

TABLE IV. EFFECT OF FAULT RESISTANCE

Fault Type	Fault Resis-tance (Ω)	Fault Applied at (km)				Error (%)
		60	120	240	300	
A-G	0	60.01	120.03	241.86	300.01	0.62
	25	60.01	120.03	241.86	301.86	0.62
	50	61.87	120.03	241.86	301.86	0.62
AB-G	0	60.01	120.03	240.06	300.01	0.02
	25	60.01	120.03	240.03	301.86	0.62
	50	60.01	120.03	240.03	301.86	0.62
ABC-G	0	60.01	120.03	241.86	300.01	0.62
	25	60.01	120.03	241.86	301.86	0.62
	50	60.01	121.86	240.03	301.86	0.62
AB	0	60.01	120.03	240.03	300.01	0.02
	25	60.01	121.86	240.03	301.86	0.62
	50	60.01	120.03	241.86	301.86	0.62

D. Case IV: Fault Inception Angle

The fault inception angle may have some influence on calculating the distance to the fault. Several values of inception angle, shown in Table V, were used in order to analyze its effect.

The results suggest that the fault inception angle has a negligible impact in calculating the distance at which the fault occurs since a small magnitude of the traveling wave is required for fault detection and localization. For smaller fault inception angles, a technique described in [22] and based on current measurements can also be applied

TABLE V. EFFECT OF FAULT INCEPTION ANGLE

Fault type	Fault inception angle (radians)	Fault applied at (km)			
		60	120	240	300
A-G	π/20	60.01	120.03	241.86	300.01
	π/5	60.01	120.03	241.86	300.01
	2π/5	60.01	120.03	241.86	300.01
	3π/5	60.01	120.03	241.86	300.01
	4π/5	60.01	120.03	241.86	300.01
AB-G	π/20	60.01	120.03	240.06	300.01
	π/5	60.01	120.03	240.06	300.01
	2π/5	60.01	120.03	240.06	300.01
	3π/5	60.01	120.03	240.06	300.01
	4π/5	60.01	120.03	240.06	300.01
ABC-G	π/20	60.01	120.03	241.86	300.01
	π/5	60.01	120.03	241.86	300.01
	2π/5	60.01	120.03	241.86	300.01
	3π/5	60.01	120.03	241.86	300.01
	4π/5	60.01	120.03	241.86	300.01
AB	π/5	60.01	120.03	240.06	300.01
	π/5	60.01	120.03	240.06	300.01
	2π/5	60.01	120.03	240.06	300.01
	3π/5	60.01	120.03	240.06	300.01
	4π/5	60.01	120.03	240.06	300.01

E. Case V: Different load and operating conditions

The algorithm performance was analyzed with different load and operating conditions. In particular, two sceneries are analyzed: changes on load magnitude and power factor. Under these varied conditions the performance of relay *R* at bus 1 was evaluated, see Fig. 2. Table VI shows the results of these simulations for an A-G fault applied at several distances along the line between buses 1 and 6. Observe that the error in the calculated distance to the fault is smaller than 0.7%, which demonstrate that the algorithm

performance is not affected by these varied conditions.

TABLE VI. EFFECT OF DIFFERENT LOAD CONDITIONS

Power Factor	Load (MVA)	Fault Applied at (km)				Error (%)
		60	120	240	300	
0.95	440	60.01	120.03	241.86	300.01	0.62
	340	60.01	120.03	241.86	300.01	0.62
	240	60.01	120.03	241.86	300.01	0.62
0.9	440	60.01	120.03	241.86	300.01	0.02
	340	60.01	120.03	241.86	300.01	0.62
	240	60.01	120.03	241.86	300.01	0.62

V. CONCLUSION

In the last decades, the growth of power electronic devices in power transmission networks has been increased significantly. Some of these devices produce diverse and sometimes undesirably effects in other control, measuring and protection systems. The SSSC performance during fault events is of particular interest because it modifies the impedance seen by conventional distance relays.

This paper proposes a new fault detection and localization method for transmission lines compensated with a SSSC. The algorithm is based on traveling waves produced during fault events and the wavelet transform. The approach used avoids low frequency interference generated by harmonic currents generated by the SSSC. The algorithm is intended for continuous operation, detecting the occurrence of transmission line faults and its localization along the line despite the SSSC presence. The developed algorithm was embedded in a relay model and tested.

The algorithm performance was analyzed considering several scenarios where some relevant parameters are varied, and the algorithm performance evaluated. These parameters are the voltage compensation level, fault resistance and the fault inception angle.

The diverse cases of study indicate that the algorithm is accurate, and can be successfully be used for fault detection and localization in transmission lines compensated with a SSSC. The error in calculating the distance to the fault is smaller than 1.5% of the transmission line length which is considered acceptable.

REFERENCES

[1] M. Khederzadeh, T. S. Sidhu, "Impact of TCSC on the protection of transmission lines", IEEE Trans. on Power Delivery, Vol. 21, No. 1, pp. 80-87, 2006. [Online]. Available: http://dx.doi.org/ 10.1109/TPWRD.2005.858798.

[2] W. Weiguo, Y. Xianggen, Y. Jiang, D. Xianzhong, C. Deshu, "The impact of TCSC on distance protection relay", in *Proc. of Power System Technology (POWERCON) International Conference*, Beijin, 1998, pp. 382-388. [Online]. Available: http://dx.doi.org/ 10.1109/ICPST.1998.728991.

[3] A. Kazemi, S. Jamali and H. Shateri, "Effects of STATCOM on Distance Relay Tripping Characteristic", *IEEE Transmission and Distribution Conference and Exposition*, Dalian, 2005, pp. 1-6. [Online]. Available: http://dx.doi.org/ 10.1109/TDC.2005.1547111.

[4] Z. Wen-Hao, L. Seung-Jae, C. Myeon-Song, O. Shigeto, "Considerations on Distance Relay Setting for Transmission Line with STATCOM", In IEEE Power and Energy Society General Meeting, Minneapolis, MN, 2010, pp. 1-5. [Online]. Available: http://dx.doi.org/ 10.1109/PES.2010.5588192.

[5] A. Kazemi, S. Jamali and H. Shateri, "Effects of SMES Equipped SSSC on Distance Relay Tripping Characteristic", IEEE Transmission and Distribution Conference and Exposition, Chicago, IL, 2008, pp. 1-6. [Online]. Available: http://dx.doi.org/ 10.1109/TDC.2008.4517157.

[6] S. Jamali, A. Kazemi and H. Shateri, "Distance Relay Over-Reaching due to SSSC Presence on Second Circuit of Double Circuit Line", In proceedings of 3rd IEEE Conference on Industrial Electronics and Applications (ICIEA 2008), Singapore, 2008, pp. 918-923. [Online]. Available: http://dx.doi.org/ 10.1109/ICIEA.2008.4582649.

[7] A. Ghorbani, B. Mozafari, A. M. Ranjbar, "Digital distance protection of transmission lines in the presence of SSSC", International Journal of Electrical Power & Energy Systems, Vol. 43, pp. 712-719, 2012. [Online]. Available: http://dx.doi.org/ 10.1016/j.ijepes.2012.05.035.

[8] Q. Xuanwei, W. Minghao, Y. Xianggen, Z. Zhe, T. Jinrui, C. Fei, "A novel fast distance relay for series compensated transmission lines", International Journal of Electrical Power & Energy Systems, Vol. 64, pp. 1-8, 2015. [Online]. Available: http://dx.doi.org/ 10.1016/j.ijepes.2014.07.028.

[9] A.M. El-Zonkoly and H. Desouki, "Wavelet entropy based algorithm for fault detection and classification in FACTS compensated transmission line", International Journal of Electrical Power & Energy Systems, Vol 33, No.8, pp. 1368-1374, 2011. [Online]. Available: http://dx.doi.org/ 10.1016/j.ijepes.2011.06.014.

[10] M. Sedighizadeh, A. Rezazadeh, I. Elkalashy, "Approaches in High Impedance Fault Detection A Chronological Review", Advances in Electrical and Computer Engineering (AECE), Vol. 10, No. 3, pp. 114-128, 2010. [Online]. Available: http://dx.doi.org/ 10.4316/AECE.2010.03019.

[11] G. Mahmoud, I. Doaa, and E. El Sayed, "Traveling-Wave-Based Fault-Location Scheme for Multiend-Aged Underground Cable System", IEEE Trans. on Power Delivery, Vol. 22, No.1, pp. 82-89, 2007. [Online]. Available: http://dx.doi.org/ 10.1109/TPWRD.2006.881439.

[12] N. Ghaffarzadeh and B. Vahidi, "A New Protection Scheme for High Impedance Fault Detection using Wavelet Packet Transform", Advances in Electrical and Computer Engineering (AECE), Vol. 10, No. 3, pp. 17-20, 2010. [Online]. Available: http://dx.doi.org/ 10.4316/AECE.2010.03003.

[13] P.K. Dash, J. Moirangthem and S. Das, "A new time-frequency approach for distance protection in parallel transmission lines operating with STATCOM", International Journal of Electrical Power & Energy Systems, Vol. 61, No. 9, pp. 606-619, 2014. [Online]. Available: http://dx.doi.org/ 10.1016/j.ijepes.2014.04.011.

[14] P.K. Dash and S.R. Samantaray. "Phase selection and fault section identification in thyristor controlled series compensated line using discrete wavelet transform". International Journal of Electrical Power & Energy Systems, Vol. 26, No. 9, pp. 725-732, 2004. [Online]. Available: http://dx.doi.org/ 10.1016/j.ijepes.2004.05.005.

[15] K. K. Sen, "SSSC - Static Synchronous Series Compensator: Theory, Modeling, and Applications", IEEE Trans. on Power Delivery, Vol. 13, No. 1, pp. 241-246, 1998. [Online]. Available: http://dx.doi.org/ 10.1109/61.660884.

[16] M. Pourahmadi-Nakhli, A.A. Safavi, "Path Characteristic Frequency-Based Fault Locating in Radial Distribution Systems Using Wavelets and Neural Networks", IEEE Trans. on Power Delivery, Vol. 26, No.2, pp. 772-781, 2011. [Online]. Available: http://dx.doi.org/ 10.1109/TPWRD.2010.2050218.

[17] S. Jiang S, U.D. Annakkage, A.M. Gole, "A Platform for Validation of FACTS Models", IEEE Trans. on Power Delivery, Vol. 21, pp. 484-491, 2006. [Online]. Available: http://dx.doi.org/ 10.1109/TPWRD.2005.852301.

[18] N. Hingorani and L. Gyugyi, "Understanding FACTS", New York USA: IEEE PRESS, pp. 74-80, 2000.

[19] A. Abur and F.H. Magnago, "Use of time delays between modal components in wavelet based fault location", International Journal of Electrical Power & Energy Systems, Vol. 22, No. 6, pp. 397-403, 2000. [Online]. Available: http://dx.doi.org/ 10.1016/S0142-0615(00)00010-7.

[20] N. Perera, A.D. Rajapakse. "Fast isolation of faults in transmission systems using current transients". Electric Power Systems Research, Vol. 78, No. 9, pp. 1568-1578, 2008. [Online]. Available: http://dx.doi.org/ 10.1016/j.epsr.2008.01.018.

[21] N. El Halabi, M. García-Gracia, S. M. Arroyo and A. Alonso, "Application of a distance relaying scheme to compensate fault location errors due to fault resistance", Electric Power Systems Research, Vol. 81, pp. 1681-1687, 2011. [Online]. Available: http://dx.doi.org/ 10.1016/j.epsr.2011.04.001.

[22] M. García-Gracia, A. Montañés, N. El Halabi and M.P. Comech, "High resistive zero-crossing instant faults detection and location scheme based on wavelet analysis", Electric Power Systems Research, Vol. 92, pp. 138-144, 2012. [Online]. Available: http://dx.doi.org/ 10.1016/j.epsr.2012.06.005.